

## Original article

# R wave detection using fractional digital differentiation

Y. Ferdi <sup>a,\*</sup>, J.P. Herbeuval <sup>b</sup>, A. Charef <sup>c</sup>, B. Boucheham <sup>d</sup><sup>a</sup> *Département d'Electrotechnique, Université de Skikda, B.P. 26, Route d'El Hadaiek, Skikda, Algeria*<sup>b</sup> *CRAN-ENSEM-INPL, 2, Avenue de la Forêt de Haye, 54516 Vandœuvre-lès-Nancy, France*<sup>c</sup> *Département d'Electronique, Université de Constantine, Route d'Ain El Bey, Algeria*<sup>d</sup> *Département d'Informatique, Université de Skikda, B.P. 26, Route d'El Hadaiek, Skikda, Algeria*

Received 14 May 2002; accepted 19 August 2003

## Abstract

In this paper, a fractional digital differentiation-based algorithm for detecting R wave in QRS complex of electrocardiogram (ECG) is developed. A FIR bandpass filter, whose coefficients only depend on fractional orders, reduces various noises present in ECG signals and generates peaks corresponding to the ECG parts with high slopes. This filter is followed by nonlinear transforms and smoothing to enhance peaks corresponding to R waves. Algorithm tests on the Massachusetts Institute of Technology/Beth Israel Hospital (MIT/BIH) ECG database illustrate the capability of this novel approach to recognizing QRS complexes in very noisy ECG signals. The algorithm's performances are comparable to those of the most efficient QRS detectors tested on this database.

© 2003 Éditions scientifiques et médicales Elsevier SAS. All rights reserved.

## Résumé

Détection de l'onde R par application de la dérivation numérique fractionnaire. Nous présentons dans cet article un algorithme fondé sur la dérivation numérique fractionnaire pour la détection de l'onde R dans le signal électrocardiographique (ECG). Un filtre passe bande, de type RIF, dont les coefficients ne dépendent que des ordres fractionnaires, réduit divers bruits de l'ECG et génère des pics plus marqués correspondant aux segments de l'ECG présentant de fortes pentes. Ce filtre est suivi de transformations non linéaires et d'opérations de lissage pour mieux mettre en évidence les pics correspondant aux ondes R. Les tests de cet algorithme sur les signaux ECG de la base de données du Massachusetts Institute of Technology/Beth Israel Hospital (MIT/BIH) *arrhythmia database* illustrent les capacités de cette nouvelle approche à reconnaître les complexes QRS de signaux ECG fortement bruités. Les performances de cet algorithme sont comparables à celles des détecteurs de QRS les plus performants testés sur cette base de données.

© 2003 Éditions scientifiques et médicales Elsevier SAS. All rights reserved.

**Keywords:** Electrocardiogram; Fractional differentiation; Fractal model; QRS detection

**Mots clés :** Electrocardiogramme ; Dérivation fractionnaire ; Détection de complexe QRS ; Modèle fractal

## 1. Introduction

Algorithm for detecting R wave in QRS complex of electrocardiogram (ECG) has many applications including R–R interval analysis, ST-segment examination, ECG compression and ECG waveform classification. Many software QRS detectors are described in the literature [1–7]. Generally, raw ECG undergoes a bandpass (or matched) filtering to suppress

noise, P and T waves, and a differentiation to emphasize large slope of R wave. To enhance QRS complexes, the filtered ECG is then passed through a nonlinear transformation such as rectification and squaring. The output of this processing is finally examined using decision rules to assert the occurrence of QRS complexes. Common QRS decision rules components are detection threshold, blanking, where events occurring after a QRS detection are ignored for a time equal to a refractory period, and search back, where previously rejected events are reexamined when a significant time has passed without finding a QRS complex.

\* Corresponding author.

E-mail address: [yferdi@yahoo.fr](mailto:yferdi@yahoo.fr) (Y. Ferdi).

The main challenge for QRS detectors is noise often present in ECG signals, particularly ambulatory and exercise ECG. The noise in ECG originates from various sources, which includes muscular activity, movements artifacts, power line interference, poor electrode contact and baseline wandering due to respiration [8]. Even P and T waves with high amplitude may be considered as challenging noise as they hinder R wave detection.

Fractional digital differentiation has proved to be robust with regard to noise in image processing [9] as well as in ECG signal processing [10]. This feature is due to lowpass differentiation property when the fractional order is negative; lowpass filtering and characteristic points (inflection points and extrema) detection are performed in the same time.

The QRS complex detection algorithm described in this paper uses a fractional digital differentiation-based filter whose coefficients depend only on fractional orders. Fig. 1 shows the block diagram of the R wave detection algorithm. The various steps are described in detail in the following sections. Tests of the algorithm on the Massachusetts Institute of Technology/Beth Israel Hospital (MIT/BIH) ECG database, prove its high performance with very noisy ECG signals.

## 2. Bandpass filtering

A FIR bandpass filter based on fractional digital differentiation has been designed [10]. This filter performs differentiation and filtering of the electrocardiographic (ECG) signal in one step by choosing appropriate fractional orders. Fig. 2 shows the block diagram of this filter. It is implemented by cascading two filters, each resulting from the difference of forward and backward truncated temporal fractional deriva-

tive. The backward time fractional derivative and forward time fractional derivative are, respectively, given by Oustaloup [9]

$$y_b(k) = \frac{1}{T_s^n} \sum_{i=0}^{\infty} a_i x(k-i) \quad (1)$$

$$y_f(k) = \frac{1}{T_s^n} \sum_{i=0}^{\infty} a_i x(k+i) \quad (2)$$

where  $x(k)$  are samples of the ECG signal sampled with period  $T_s$ ,  $n$  is the fractional order of differentiation ( $n > 0$ ) or integration ( $n < 0$ ) and  $a_i$  are expansion coefficients of the series  $(1-Z)^n$ . The coefficients  $a_i$  are given by

$$a_0 = 1 \text{ and } a_i = \frac{i-n-1}{i} a_{i-1}, \quad i = 1, 2, 3, \dots \quad (3)$$

The low frequency residual noise is reduced by the second filter with positive fractional order. Each output filter ( $n = n_1$  or  $n_2$ , see Fig. 2) can be written as follows:

$$y(k) = \sum_{i=-\infty}^{\infty} h(i)x(k-i) \quad (4)$$

with

$$h(i) = \begin{cases} -\frac{a_i}{T_s^n}, & i = 1, 2, \dots \\ 0, & i = 0 \end{cases} \quad (5)$$

and

$$h(-i) = -h(i) \quad (6)$$

$h(i)$  can be considered as the discrete-time noncausal antisymmetric impulse response of the system. We truncate the sequence  $h(i)$  between  $-(M-1)/2$  and  $(M-1)/2$ , where  $M$



Fig. 1. Block diagram of the R wave detector.

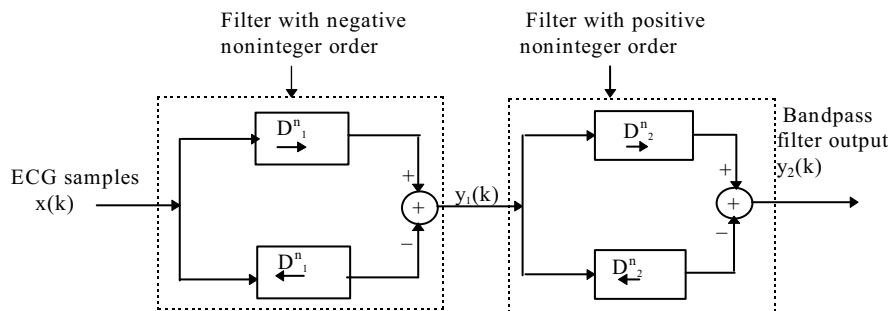


Fig. 2. Bandpass filter block diagram. Top path: forward time fractional derivative. Bottom path: backward time fractional derivative.

is an odd integer. Under these circumstances, we obtain a FIR filter whose amplitude response is given by

$$H_M(jf) = 2j \sum_{i=1}^{(M-1)/2} h(i) \sin(2\pi f i T_s) \quad (7)$$

The two filters series combination of transfer functions (7) with fractional orders, respectively, negative and positive forms a bandpass filter whose central frequency is determined by the values of  $M$ ,  $n_1$  and  $n_2$ ;  $n_1$  denotes the negative order and  $n_2$  the positive order. We select the  $M$  value and the negative order  $n_1$  of fractional differentiation such that the signal (QRS complex) to noise ratio is maximized. We consider that the high frequency noise that affects the ECG essentially originates from the muscular activity (EMG) whose power spectral density is constant [11]. The power spectral density of the QRS complex studied by Goldberger et al. [12] and estimated by Thakor et al. [11], was modeled by a linear approximation by Laguna et al. [13]. It was modeled by Sun and Charef [14] by the following fractal

model:  $S_{QRS}(f) = \frac{K}{(4\pi^2 f^2 + p^2)^\beta}$  where  $\beta = 2.1$  and  $p = 8\pi$  rad/s. (8)

The signal to noise ratio was computed using the following relation:

$$SNR_M(n_1) = \frac{\int_0^{f_{\max}} S_{QRS}(f) |H_M(f)|^2 df}{N_0 \int_0^{1/2T_s} |H_M(f)|^2 df} \quad (9)$$

as function of the fractional order  $n_1$  with  $M$  as parameter.  $f_{\max}$  represents the QRS complex bandwidth and  $N_0$  the spectral density of the EMG. The value of positive order  $n_2$  is mainly selected on the basis of its effects on the center frequency of the bandpass filter and on the amplification of noises.  $n_2$  has minor influence on the center frequency lying between 10 and 25 Hz as reported in literature. However,  $n_2$  effect on noise amplification is more marked and must be kept at an acceptable level. In this study, we selected  $n_2 = 0.2$ .

Corresponding to  $n_2 = 0.2$  and different values of  $n_1$  and  $M$ , the amplitude frequency responses of the bandpass filter are shown in Fig. 3. The sampling rate of the ECG is 360 Hz. The center frequency is 29.5, 25, 21.5 and 19 Hz, respectively, for  $M = 11$  and  $n_1 = -0.33$ ,  $M = 13$  and  $n_1 = -0.38$ ,  $M = 15$  and  $n_1 = -0.43$ ,  $M = 17$  and  $n_1 = -0.46$ .

Fig. 4 illustrates the responses of the bandpass filter to two ECG cycles simulated by gaussian pulses [15]. The first cycle is noise free but the second is corrupted by an abrupt wander of the baseline. One can see in Fig. 4(b) that the R wave corresponds to a pair of pulses located on either side of the time axis but the abrupt deviation of the baseline gives rise to a uniphase wave.

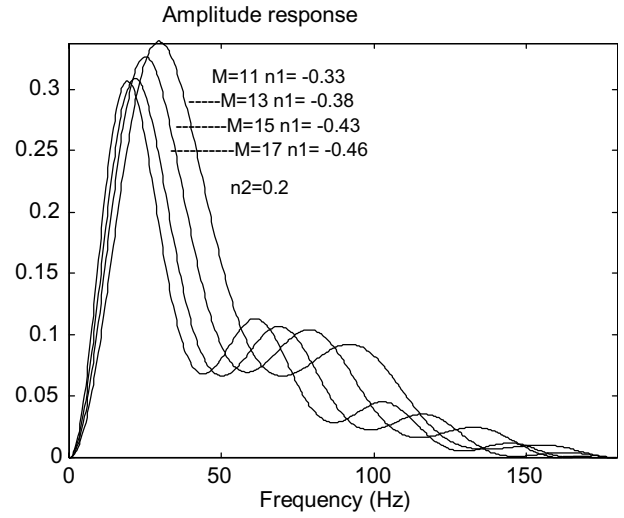


Fig. 3. Amplitude frequency responses of the bandpass filter for different values of  $M$ ,  $n_1$  and  $n_2$ . Sampling rate  $F_s = 360$  Hz.

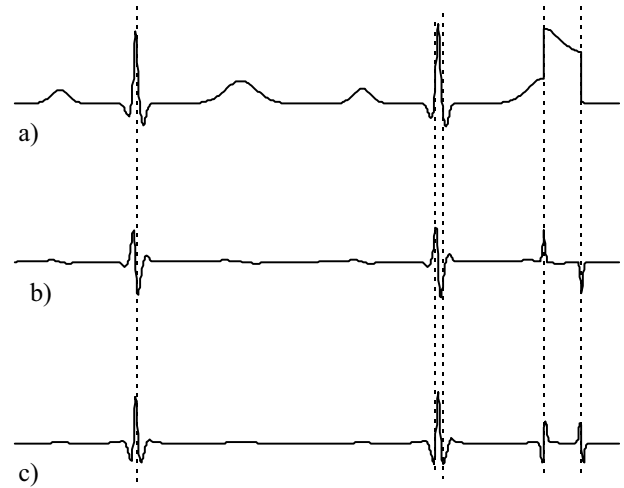


Fig. 4. Bandpass filter output to simulated ECG. a) original signal; b) output of the filter with negative order; c) bandpass filter output

### 3. Bandpass filter implementation

We have exploited the recursion property of the binomial coefficients to avoid their explicit calculation. The response of each filters ( $n = n_1$  or  $n_2$ ) is then written as follows:

$$y(k) = \frac{1}{(T_s)^n} \left\{ -n \left\{ u(k-1) + \frac{1-n}{2} \right. \right. \\ \left. \left\{ u(k-2) + \dots + \frac{(M-5)/2-n}{(M-3)/2} \left\{ u\left(k+1 - \frac{M-1}{2}\right) + \right. \right. \right. \\ \left. \left. \frac{(M-1)/2-n-1}{(M-1)/2} u\left(k - \frac{M-1}{2}\right) \right\} \dots \right\} \right\} \quad (10)$$

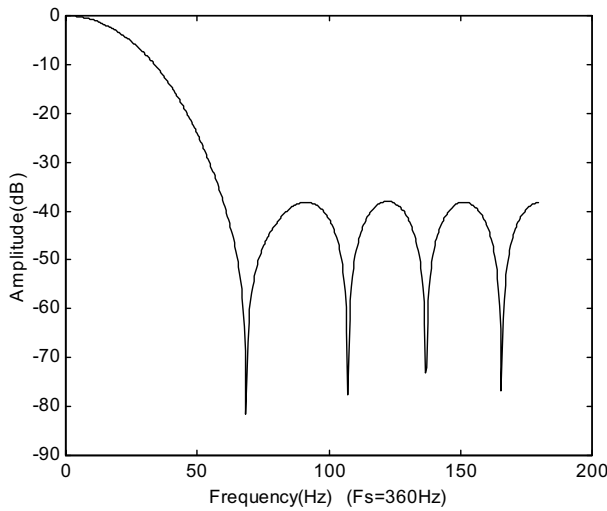


Fig. 5. Amplitude frequency response of the smoothing filter with  $N = 13$ .

with

$$u(k-i) = x(k+i) - x(k-i), \quad i = 1, 2, \dots, \frac{M-1}{2} \quad (11)$$

This relation avoids the storage of the coefficients in memory.

#### 4. Nonlinear transforms and smoothing

The signal to be compared to an adaptive threshold has been generated using the following scheme:

1. rectification (absolute value) of the responses  $y_1(k)$  and  $y_2(k)$  of the two filters;
2. smoothing of the rectified signals  $y_1(k)$  and  $y_2(k)$  by a lowpass filter which has been designed using the non-integer derivative relation (1) with  $n = -1$  and truncated to  $N$  terms. To reduce the oscillations owing to the truncation, we multiply the derivative by Hamming window function:

$$w(k) = 0.54 - 0.46 \cos \frac{2\pi k}{N-1}, \quad 0 \leq k \leq N-1 \quad (12)$$

According to the power spectra of the ECG signal, artifacts and noises [11], a filter having a  $-3$  dB cutoff frequency of 20 Hz, that is  $N = 13$ , appears to be a good compromise between the alteration of QRS complex peaks and the noise attenuation. Fig. 5 shows the amplitude frequency response of this filter;

3. Multiplication of the rectified and smoothed signals  $y_1(k)$  and  $y_2(k)$ . Their product is squared and then smoothed using the filter of step 2. The squaring aims to enhance the peaks corresponding to QRS complexes.

We note that the smoothing filter introduces a delay of  $(N-1)/2$  samples that we corrected after we applied the filter to the data.

#### 5. Application to noisy ECG signals

We applied, with no preprocessing, different segments of ECG taken from MIT/BIH arrhythmia database to the input of the bandpass filter of Fig. 2 with  $M = 17$ ,  $n_1 = -0.46$  and  $n_2 = 0.2$ . The MIT/BIH database, recorded on a CD-ROM, contains twin channel ECG waveforms of about 30 min each from 48 patients (two leads per patients). The sampling frequency is 360 Hz. ECG segments, that contain 2500 samples each, are taken from the first channel of the registration. In each of Figs. 6–8, the waveforms (a) represent the original signals ECG. The waveforms (b) and (c) show the filters responses, respectively, with negative and positive order. The signal (d) is the sequence to be threshold compared (STC).

The ECG in Fig. 6 includes a gradual deviation of the baseline. One can also see an important amplitude variation of the QRS complexes. The QRS of weak amplitudes are strongly attenuated in signal (d), but keep some sufficient amplitude to be detected from signal (c). In Fig. 7, the ECG is corrupted by an abrupt jump of the baseline. The ECG shown in Fig. 8 includes premature ventricular contraction (PVC) morphology. We note the ability of the algorithm to enhance the QRS complexes despite the presence in the ECG of noise waves-like QRS complex.

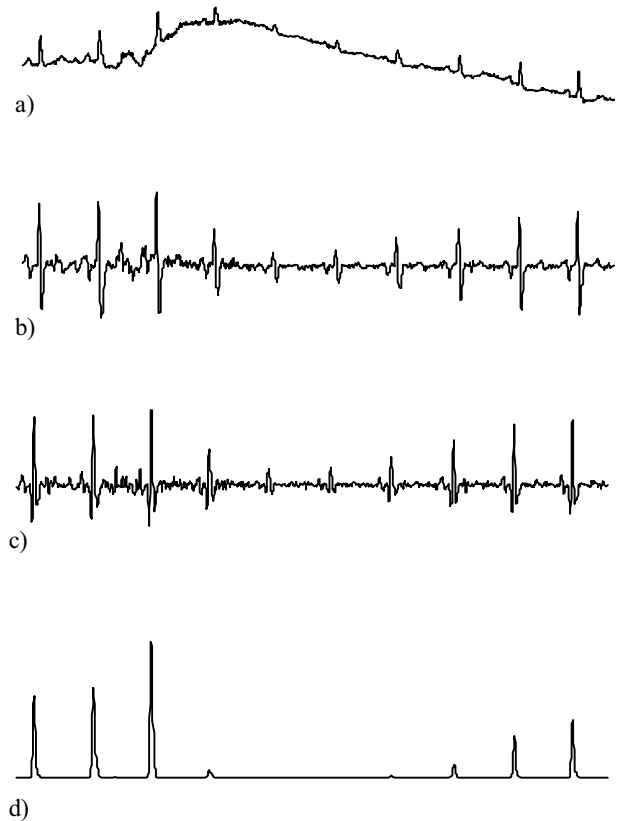


Fig. 6. ECG with gradual deviation of the baseline (Record 105).

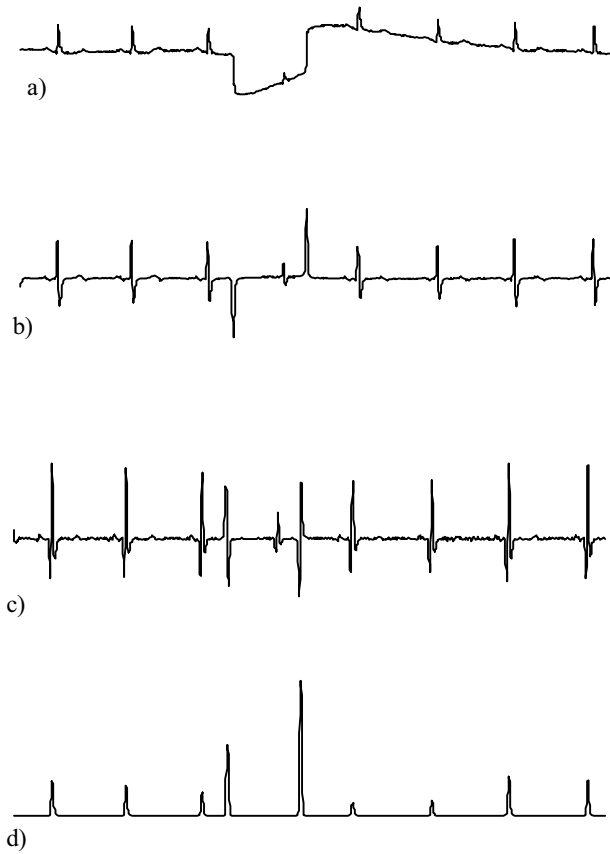


Fig. 7. ECG with abrupt deviation of the baseline (Record 101).

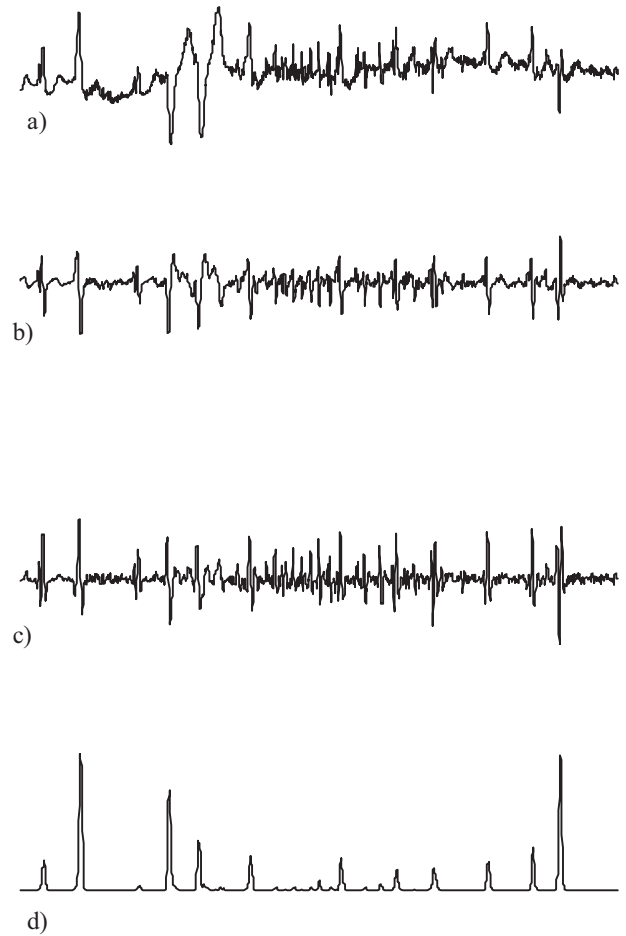


Fig. 8. ECG with high frequency noise and PVC (Record 203).

## 6. R peak detection procedure

The ECG signals we used in this paper are ambulatory recordings. In these signals, complex QRS amplitude can vary considerably within a short interval of time. This requires using an adaptive detection threshold according to the following relationship

$$\text{detectionthreshold} = C_1 \times \text{Estimate} \quad (13)$$

where *estimate* is the amplitude value of the (STC) peak and  $C_1$  is the threshold coefficient. *estimate* may be computed by one of three estimators: mean, median or iterative [5]. In the initialization stage, *estimate* is obtained by the (STC) maximum value in a sufficient wide window, which contains at least one QRS complex.

When the (STC) amplitude reaches the detection threshold, the algorithm begins searching for the instant  $t_{y_{\max}}$  of its maximum value in an interval whose width is less than half of the widest QRS width. Then, a window whose width is less than that of widest QRS and centered at  $t_{y_{\max}}$  is used to search for the maximum value instant  $t_{y_{2\max}}$  of the waveform  $y_2(k)$ , rectified and smoothed. The  $t_{y_{2\max}}$  instant is then used as middle of a window where the algorithm will search for the maximal value and the minimal value of the response  $y_1(k)$  of

the filter with negative order. The instant  $t_{y_{2\max}}$  will be considered as the R wave occurrence instant if the two following conditions are met:

1. the time interval between maximum and minimum values of  $y_1(k)$  is less than the duration of widest QRS complex (Fig. 4b);
2. the two extreme values of  $y_1(k)$  are located on either side of the time axis. The false positive (false detection) caused by abrupt fluctuations of the baseline are thus eliminated.

Some QRS complex widen, as in branch block, can have lengths going up to 120 ms [16]. This value has been selected as threshold for widest QRS complex in this paper. The sampling frequency being 360 Hz, this threshold corresponds, therefore, to 43 samples. After detection of a QRS complex, all events detected before the end of the refractory period of 200 ms, will be ignored.

In spite of the use of an adaptive detection threshold, some QRS complexes may be missed by the detector. This non-detection is marked by the algorithm by measuring the time elapsed since the last QRS detection. If the measured value is superior to 150% of the R–R interval estimated by a 8-point median estimator, the algorithm will perform a search back

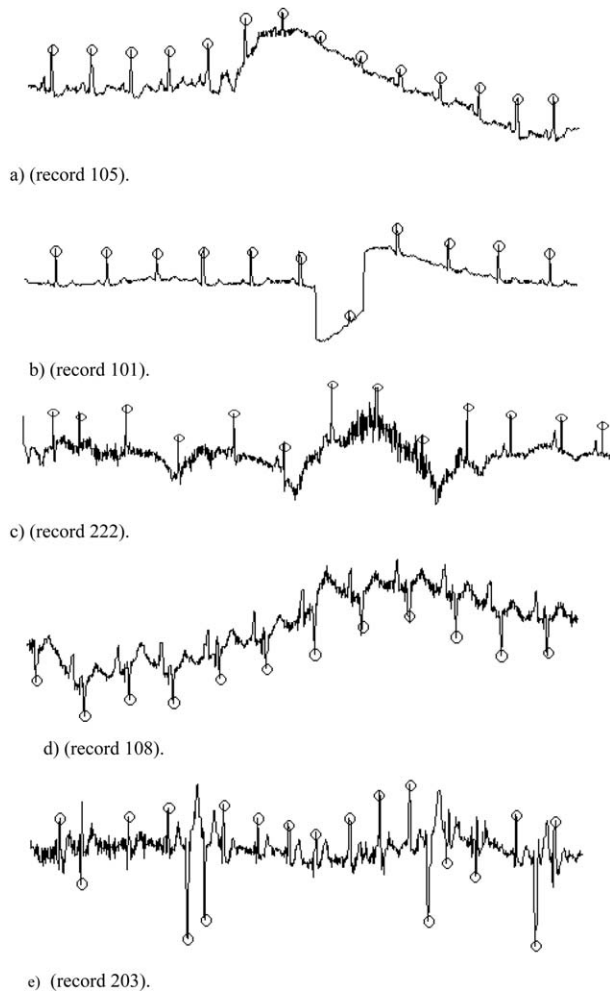


Fig. 9. The detected R waves. The small circle marks the locations of R peaks; a) gradual deviation of the baseline; b) abrupt deviation of the baseline; c) noise like QRS complex; d) high amplitude P wave, e) high amplitude T wave.

on  $y_2(k)$ , smoothed and rectified, with a new detection threshold given by

$$\text{detection threshold} = C_2 \times y_{2\max} \quad (14)$$

where  $y_{2\max}$  is the maximum value of  $y_2(k)$  smoothed and rectified corresponding to last detected QRS. The selection of the 8-points median estimator to estimate the R–R interval is based on Hamilton and Tompkins survey results [5].

The instants corresponding to R wave occurrences are saved in files. The contents of these files will be compared to those of records annotations files during the algorithm evaluation procedure on MIT/BIH arrhythmia database ECG signals.

Fig. 9a–e show examples of QRS complex detection by the proposed algorithm. The small circles on signals correspond to R waves. The chosen examples include the current artifacts, P and T waves with high amplitudes that cause QRS bad detection when the analysis of the ECG is done by computer. These examples illustrate the capabilities of our algorithm to detect QRS complexes with various morpho-

Table 1

Results of evaluation of QRS detector based on fractional digital differentiation using MIT/BIH arrhythmia database

Record N°	Total (beats)	FP (beats)	FN (beats)	Failed detection (FP + FN)	Failed detection (%) (FP + FN) × 100/Total
100	2273	0	1	1	0.04
101	1865	0	0	0	0.00
102	2187	4	0	4	0.18
103	2084	0	0	0	0.00
104	2229	6	5	11	0.49
105	2572	16	14	30	1.17
106	2027	3	8	11	0.54
107	2137	3	5	8	0.37
108	1763	21	25	46	2.61
109	2532	7	6	13	0.51
111	2124	6	2	8	0.38
112	2539	0	0	0	0.00
113	1795	0	1	1	0.06
114	1879	8	12	20	1.06
115	1953	0	0	0	0.00
116	2412	0	12	12	0.50
117	1535	0	0	0	0.00
118	2278	0	0	0	0.00
119	1987	8	8	16	0.81
121	1863	2	1	3	0.16
122	2476	0	0	0	0.00
123	1518	0	3	3	0.20
124	1619	0	2	2	0.12
200	2601	1	2	3	0.12
201	1963	6	12	18	0.92
202	2136	1	2	3	0.14
203	2980	4	17	21	0.70
205	2656	0	4	4	0.15
207	1860	6	12	18	0.97
208	2955	3	9	12	0.41
209	3004	1	1	2	0.07
210	2650	7	8	15	0.57
212	2748	0	0	0	0.00
213	3251	2	1	3	0.09
214	2261	1	3	4	0.18
215	3363	0	5	5	0.15
217	2208	2	7	9	0.41
219	2154	0	3	3	0.14
220	2048	0	1	1	0.05
221	2427	5	9	14	0.58
222	2483	5	13	18	0.72
223	2605	4	7	11	0.42
228	2053	11	12	23	1.12
230	2256	0	0	0	0.00
231	1571	0	0	0	0.00
232	1780	3	12	15	0.84
233	3079	0	8	8	0.26
234	2753	0	3	3	0.11
Totals	109492	146	256	402	0.37

Table 2

Comparison of performances for QRS complex detectors using MIT/BIH arrhythmia database

Comparison criterion	Proposed algorithm	WT	BPI	BPII
Number of false positive (beats)	146	65	248	507
Number of false negative (beats)	256	112	340	277
Failed detection rate (%)	0.37	0.15	0.54	0.68



Table 3  
Comparison of performances for QRS complex detectors for the most noisy records 105 and 108

Comparison criterion	Proposed algorithm		ANN		WT		BPI		BPPI	
	105	108	105	108	105	108	105	108	105	108
Number of false positive (beats)	16	21	10	25	15	13	53	50	67	199
Number of false negative (beats)	14	25	4	16	13	15	22	47	22	22
Failed detection rate (%)	1.17	2.61	0.50	2.32	1.09	1.59	2.95	5.67	3.46	12.54

gies in ECG corrupted by different artifacts, P and T waves with high amplitudes.

## 7. Performance evaluation

The performance of QRS detector is usually measured in terms of the number of QRS complexes missed (false negative: FN) and the number of QRS complexes falsely reported (false positive: FP) for a given set of parameters [1,2,4,5,6]. There are five parameters ( $M$ ,  $n_1$ ,  $n_2$ ,  $C_1$  and  $C_2$ ) within our algorithm. The values of  $M$ ,  $n_1$  and  $n_2$  are determined as explained above. For the selection of the detection threshold coefficients  $C_1$  and  $C_2$ , we performed a set of trials with  $C_2$  fixed and  $C_1$  varied from 0.1 to 0.9. To avoid false detection in searching back procedure,  $C_2$  must be chosen relatively high (say greater than 0.5) since missed QRS peaks may be easily confused with noise peaks. We selected  $C_2 = 0.65$ . In a first experiment, we used median estimator. The 48 records of the MIT/BIH database are analyzed separately nine times with  $C_1$  ranging from 0.1 to 0.9. For each trial, the failed detection rate defined by  $(FP + FN) \times 100 / (\text{total number of beats})$  is computed. Two other experiments using mean estimator and iterative estimator are then performed. The obtained results are dependent of the analyzed record and the estimator type. In this paper, we selected  $C_1$  as the mean of the 48 optimal values corresponding to lower failed detection rates for each record. For the three estimator, the mean value of  $C_1$  is approximately 0.3.

In evaluating our algorithm on the 48 ECG records of the MIT/BIH arrhythmia database, the three estimators are used with the following number of data points and coefficient: 8-points mean estimator, 8-points median estimator and iterative estimator with  $\alpha = 0.125$ . The R peaks instants obtained by the algorithm are compared with the corresponding contents of the associated annotation file. The best results corresponding to lower failed detection rate, obtained with 8-points mean estimator, are reported in Table 1. The algorithm was implemented on a Pentium 233 MHz personal computer with Matlab.

## 8. Comparison to other algorithms

We compared the performance of our algorithm with four QRS complex detectors reported in the literature. These are all tested on ECG signals of the MIT/BIH arrhythmia database. As it is reported, the performance of the algorithm

based on wavelet transforms (WT) [1] is superior to those of the other detectors when the 48 records are considered. The neural-network-based adaptive filtering algorithm (ANN) [4] is evaluated only on records 105 and 108. The two other detectors, based on classical bandpass filtering (BPI) [5] and (BPPI) [6], are less efficient. The results of evaluation of the QRS detectors are listed in Table 2. Comparing these results, we note that the performance of the proposed algorithm are comparable to those of the most efficient detectors, especially concerning the most noisy records, namely records 105 and 108. For these records, the reported results are given in Table 3.

## 9. Conclusion

We proposed a fractional digital differentiation-based algorithm for R wave detection of very noisy ECG signals. The algorithm was tested, in this study, on several segments from MIT/BIH arrhythmia database. These segments are corrupted by different noises and artifacts. The R wave is located despite the presence of these noises. Its performance is evaluated in terms of false positive and false negative on the ECG signals of the MIT/BIH arrhythmia database. The obtained results showed that the performances of our algorithm are comparable to the most efficient QRS complex detector tested on the same ECG signals. Furthermore, our algorithm could be implemented more easily comparatively to other algorithms based on wavelet transform or neural network.

## References

- [1] Li C, Zheng C, Tai C. Detection of ECG characteristic points using wavelet transforms. *IEEE Trans Biomed Eng* 1995;42:21–8.
- [2] Henry D, Claudon L, Robert M, Lee C. Détection de complexes QRS: une étude comparative et un nouvel algorithme basé sur le test du khi2. *ITBM* 1993;14:672–80.
- [3] Panoulas KI, Hadjileontiadis LJ, Panas SM. Enhancement of R-wave detection in ECG data analysis using higher-order statistics. *Proceedings of the Twenty third Annual Conference—IEEE/EMS, Istanbul, Turkey, October 25–28, 2001*.
- [4] Xue Q, Hu YH, Tompkins WJ. Neural-network-based adaptive matched filtering for QRS detection. *IEEE Trans Biomed Eng* 1992; 39:317–29.
- [5] Hamilton PS, Tompkins WJ. Quantitative investigation of QRS detection rules using the MIT/BIH Arrhythmia Database. *IEEE Trans Biomed Eng* 1986;BME-33(12):1157–65.
- [6] Pan J, Tompkins WJ. A real time QRS detection algorithm. *IEEE Trans Biomed Eng* 1985;BME-32(3):230–6.
- [7] Okada M. A digital filter for QRS complex detection. *IEEE Trans Biomed Eng* 1979;BME-26(12):700–3.

- [8] Friesen GM, Jannett TC, Jadallah MA, Yates SL, Quint HT, Nagle HT. A comparison of the noise sensitivity of nine QRS detection algorithms. *IEEE Trans Biomed Eng* 1990;7:85–98.
- [9] Oustaloup A. La dérivation non entière. Editons Hermès. 1995.
- [10] Ferdi Y, Herbeuval JP, Charef A. Un filtre numérique basé sur la dérivation non entière pour l'analyse du signal électrocardiographique. *ITBM-RBM* 2000;21:205–9.
- [11] Thakor NV, Webster JG, Tompkins WJ. Estimation of QRS complex power spectra for design of a QRS filter. *IEEE Trans Biomed Eng* 1984;BME-1(11):702–6.
- [12] Goldberger AL, Bhargava V, West BJ, Mandel AJ. On a mechanism of cardiac electrical stability. The fractal hypothesis. *Biophys J* 1985;48: 525–8.
- [13] Laguna PL, Thakor NV, Caminal P, Jane R. Low-pass differentiators for biological signals with known spectra: application to ECG signal processing. *IEEE Trans Biomed Eng* 1990;37:420–5.
- [14] Sun HH, Charef A. Fractal systems. A time domain approach. *Ann Biomed Eng* 1990;18:597–621.
- [15] Suppappola S, Sun Y, Chiaramida SA. Gaussian pulse decomposition: an intuitive model of electrocardiogram waveforms. *Ann Biomed Eng* 1997;25:252–60.
- [16] Dubin D. Lecture accéléré de l'ECG. 4<sup>ème</sup> Edition, 1997 Maloine.